

Characterization of S- T_+ Transition Dynamics via Correlation Measurements

Christian Dickel,^{1,*} Sandra Foletti,² Vladimir Umansky,³ and Hendrik Bluhm¹

¹JARA-Institute for Quantum Information, RWTH Aachen University, D-52074 Aachen, Germany

²Department of Physics, Harvard University, Cambridge, Massachusetts 02138, USA

³Braun Center for Submicron Research, Department of Condensed Matter Physics, Weizmann Institute of Science, Rehovot 76100, Israel

Nuclear spins are an important source of dephasing for electron spin qubits in GaAs quantum dots. Most studies of their dynamics have focused on the relatively slow longitudinal polarization. We show, based on a semiclassical model and experimentally, that the dynamics of the transverse hyperfine field can be probed by correlating individual Landau-Zener sweeps across the S- T_+ transition of a two-electron spin qubit. The relative Larmor precession of different nuclear spin species leads to oscillations in these correlations, whose decay arises from dephasing of the nuclei. In the presence of spin orbit coupling, oscillations with the absolute Larmor frequencies whose amplitude reflects the spin orbit coupling strength are expected.

PACS numbers: 73.63.Kv, 03.65.Yz, 76.70.Dx

Electron spins in semiconductor quantum dots have been studied much as a platform for quantum information processing. While at first it was envisioned to use single electron spins as qubits [1], it is also possible to encode a qubit in several electron spins. The experimentally most established approach is to use the singlet state S and the $m = 0$ triplet state, T_0 , of two electrons in a double quantum dot (DQD). Alternatively, it was proposed [2] to replace T_0 with the $m = 1$ state, T_+ . Coherent oscillations between these two states were observed using Landau-Zener-Stückelberg interferometry [2], and pulse sequences to control this type of qubit have been constructed [2–4]. The transition between S and T_0 is a narrow avoided crossing mediated by perpendicular effective magnetic fields arising from nuclear spins and spin orbit (SO) coupling [5]. It is thus important to understand the quantum dynamics of transitions between these two states, which, as we show here, are strongly affected by the precession of the nuclear spins in the external field. Nuclear spin effects are especially prominent in GaAs-based quantum dots, currently the most developed material system available for gated semiconductor quantum dots.

In addition to qubit control, the S- T_+ transition can be used to transfer angular momentum from the electronic system to the nuclear spins. The resulting dynamic nuclear polarization (DNP) has been instrumental in reducing dephasing [6] and achieving universal control [7] of S- T_0 qubits. Periodically traversing the crossing can be used to polarize the nuclear spins and even to suppress fluctuations via a feedback loop. Such nuclear spin control is useful for both gate defined and self assembled quantum dots [8–10]. In gated dots, the performance of such DNP schemes is currently limited by a low spin transfer probability from electrons to nuclei [6], which is poorly understood. It was observed that the electron spin flip rate exceeds the nuclear polarization rate, which may result from an additional SO spin flip channel [11–

14]. Probing the transitions between S and T_+ states and the role of SO coupling is thus also relevant for understanding the limitations of DNP methods.

Here, we present a measurement technique that probes the dynamics of the matrix element driving transitions between S and T_+ . Direct measurements of the Overhauser field have previously been used to probe fluctuations of its component parallel to the external magnetic field [6, 15]. However, the transverse part that drives the oscillations between S and T_+ exhibits faster dynamics that are harder to access. Our approach is based on correlating the outcomes of subsequent individual single shot measurements of the qubit state after Landau-Zener (LZ) transitions similar to [16]. After each LZ sweep, the state of the qubit is measured. From this data, the auto-correlation of single shot measurements is computed as a function of the time delay between them. The time resolution is only limited by the accuracy of pulse timing, but not by the required averaging time.

We will show in the following that these correlations reveal the relative nuclear spin Larmor precession and dephasing of these precessions on a μs scale. In the presence of SO coupling, the oscillations would exhibit additional frequency components. Therefore, the method can provide direct, qualitative and quantitative evidence for SO coupling. We also present proof of principle experimental results. They show nuclear spin effects but no SO coupling. We also point out that averaging the LZ transition probability over nuclear spin configurations leads to an algebraic instead of exponential dependence on the sweep rate. A SO component of the transition matrix element is not subject to this averaging and accordingly leads to more exponential behavior.

The two-electron spin qubits considered here consist of two electrons trapped in a double-well potential as seen in Fig. 1(a) formed by electrostatic gating of a two-dimensional electron gas in a GaAs/AlGaAs heterostructure. A comprehensive derivation of the relevant DQD

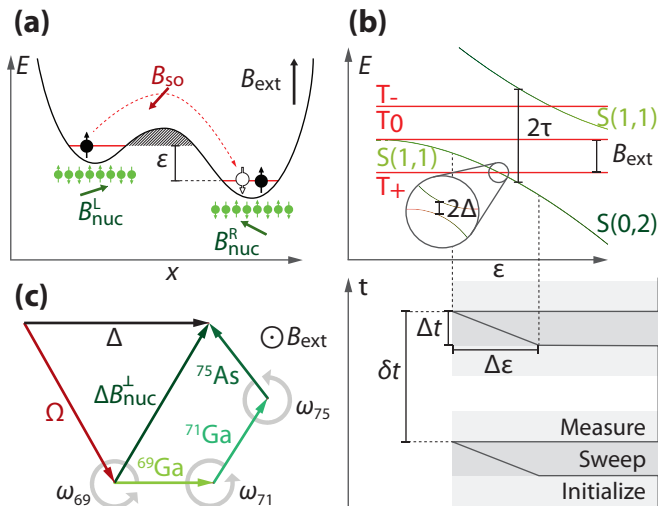


Figure 1. (a) DQD potential landscape along the dot-dot axis. Vectors indicate effective magnetic fields from SO due to tunneling and nuclear spins via the Fermi contact interaction. The detuning ε is the energy difference between the single electron levels in the dots. (b) DQD energy diagram and pulse forms for LZ correlation measurements. Pulse cycles are concatenated with a time delay δt . (c) $\Delta \mathbf{B}_{\text{nuc}}^{\perp}$ has contributions from the three different nuclear species that precess in B_{ext} with different Larmor frequencies. The S- T_+ transition matrix element Δ is a vector sum of the static SO field Ω and $\Delta \mathbf{B}_{\text{nuc}}^{\perp}$.

electronic Hamiltonian can be found in [5]. In the following we provide a qualitative summary. The qubit is controlled via the detuning, ε , defined as the energy difference between the lowest (1, 1) and (0, 2) charge configuration, where the numbers indicate the occupancy of each dot. Positive detuning favors double occupation of one dot in the singlet state, while at negative detuning the electrons are separated. The resulting level diagram as a function of ε is shown in Fig. 1(b). The singlet states exhibit an avoided crossing with tunnel coupling τ . Due to the Pauli principle, the triplet states $|T_+\rangle$, $|T_-\rangle$ and $|T_0\rangle$ with magnetic quantum numbers $m = \pm 1, 0$ always stay in the (1, 1) configuration and are energetically separated by the Zeeman energy in an external magnetic field B_{ext} . This setting allows fast electric singlet initialization and single shot readout that distinguishes singlet and triplet states via spin to charge conversion [15], independent of which triplet is used.

The focus of this Letter is the S- T_+ degeneracy point (called S- T_+ transition), where transitions between these states are possible. A convenient way to probe this narrow crossing is to employ LZ sweeps, i.e., linear sweeps across the transition as illustrated in Fig. 1(b) that do not require precise knowledge of the position of the transition. For a sufficiently small sweep range, the other states can be neglected. We use an effective Hamiltonian in the basis $\{|S^*(\varepsilon)\rangle, |T_+\rangle\}$, where $|S^*(\varepsilon)\rangle =$

$\cos \psi |S(1, 1)\rangle + \sin \psi |S(0, 2)\rangle$ is the hybridized singlet close to the crossing:

$$\mathbf{H} = \frac{B_{\text{ext}} - J(\varepsilon)}{2} \sigma_z + \Delta \sigma_x, \quad (1)$$

where σ_x and σ_z are Pauli matrices. We use units of energy for all electronic Zeeman fields, thus setting $g\mu_B = 1$. The parameters are the exchange splitting $J = E_{S^*} - E_{T_0}$ and the coupling

$$\Delta = \frac{1}{2} \left| \mathbf{B}_{\text{SO}} \sin \psi + \Delta \mathbf{B}_{\text{nuc}}^{\perp} \cos \psi \right|. \quad (2)$$

The singlet mixing angle, ψ , at the transition sets the weight of the effective SO field \mathbf{B}_{SO} , which couples $|S(0, 2)\rangle$ and $|T_+\rangle$, and the difference in transverse hyperfine fields $\Delta \mathbf{B}_{\text{nuc}}^{\perp} = (\mathbf{B}_{\text{nuc}}^{\perp, R} - \mathbf{B}_{\text{nuc}}^{\perp, L})$ between the dots, which couples $|S(1, 1)\rangle$ and $|T_+\rangle$ [5]. The mixing angle depends on τ and indirectly on B_{ext} via the position of the transition. For $J = \alpha t$, where α is the sweep rate and a sweep from $-\infty$ to ∞ , the probability that an initial singlet stays in a singlet is given by $P_S = \exp\left(-\frac{2\pi\Delta^2}{\hbar\alpha}\right)$ [17, 18].

In this work, we assume $B_{\text{ext}} \ll \tau$ so that $\cos \psi \approx 1$ and $\sin \psi \ll 1$ at the transition. $B_{\text{SO}} = \frac{4\pi}{3} \frac{l}{l_{\text{SO}}}$ depends the inter-dot distance $l \approx 200$ nm and the SO length l_{SO} [5]. Therefore the effective field from SO coupling is expected to be static with a value on the order of $B_{\text{SO}} \sim 100$ mT. For two million unit cells in each dot [19], $\left\langle (\Delta \mathbf{B}_{\text{nuc}}^{\perp})^2 \right\rangle^{1/2}$ is on the order of 4 mT. Thus even a suppressed SO coupling could approach the expected Overhauser field. We introduce the overall SO contribution to Δ , $\Omega = \mathbf{B}_{\text{SO}} \sin \psi$. In the regime of interest here, $\Omega \lesssim \left\langle (\Delta \mathbf{B}_{\text{nuc}}^{\perp})^2 \right\rangle^{1/2}$.

The dynamical effects considered here originate in the time dependence of Δ via $\Delta \mathbf{B}_{\text{nuc}}^{\perp}$, which arises from the interactions of each electron spin with on the order of 10^6 nuclear spins. As illustrated in Fig. 1(c), $\Delta \mathbf{B}_{\text{nuc}}^{\perp}$ is a vector sum of contributions from the three isotopes present in GaAs, ^{69}Ga , ^{71}Ga and ^{75}As , all with nuclear spin $3/2$. Following earlier work, we treat their fields as classical random variables [20].

In addition to the Larmor precession of the nuclei, we also account for dephasing of this precession due to microscopic field fluctuations originating from dipole-dipole interactions and quadrupole splittings. To this end, we subdivide each species into subspecies with slightly different precession frequencies $\omega_i = \gamma_i (B_{\text{ext}} + \delta B_i)$, where γ_i is the nuclear gyromagnetic ratio. The field fluctuations δB_i are taken from a discretized normal distribution with standard deviation δB_{loc} , and the index i denotes both the nuclear species and the local field value. We find that good convergence is obtained for five bins per species.

We incorporate the above dynamics by writing

$$\Delta(t)^2 = \frac{1}{4} \left(\sum_{ij} B_i^+ B_j^- e^{i(\omega_i - \omega_j)t} + \sum_i \Omega (B_i^+ e^{i\omega_i t} + B_i^- e^{-i\omega_i t}) + \Omega^2 \right), \quad (3)$$

where $B_i^\pm = B_i^x \pm iB_i^y$. Note that the contribution from SO coupling behaves like an additional, static nuclear spin species. During a single LZ sweep, we approximate Δ as constant because the nuclear spin dynamics are slow compared to the time spent at the crossing. This approximation is justified as long as $\gamma_N/\gamma_e B_{ext} \ll \Delta$, where γ_N and γ_e are nuclear and electronic gyromagnetic ratios.

The expectation values over nuclear states of the single shot measurement correlations are given by $\langle P_S(t) P_S(t + \delta t) \rangle = \left\langle \exp \left(-\frac{2\pi}{\alpha \hbar} (\Delta(t)^2 + \Delta(t + \delta t)^2) \right) \right\rangle$ [16]. To evaluate them one has to integrate over all possible initial conditions B_i^\pm . In the homogeneous coupling approximation used here, each component of the effective field of each species is approximated as normally distributed with standard deviation $B_{i,rms} = \frac{A_i}{N} \sqrt{5N_i/2}$, which corresponds to averaging over an infinite temperature nuclear ensemble. N_i is the number of spins in the i th bin, A_i the species-dependent hyperfine coupling strength and N the number of unit cells occupied by each electron.

To perform this integration, it is useful to decouple the terms via the T-matrix method [20]. The exponent of the LZ correlations is rewritten as

$$\frac{2\pi}{\hbar\alpha} \left(\Delta(t)^2 + \Delta(t + \delta t)^2 \right) = \frac{\pi}{\alpha \hbar} \Omega^2 + \sum_{ij} T_{ij}(\delta t) z_i^+ z_j^- + \sum_i V_i(\delta t)^* z_i^- + \sum_i V_i(\delta t) z_i^+$$

with $z_i = x_i + iy_i$, where x and y are normally distributed with unit variance. Diagonalizing the T-matrix, applying the same basis change to the linear terms and integrating over the z_i distributions results in

$$\langle P_S(t) P_S(t + \delta t) \rangle = \exp \left(-\frac{\pi \Omega^2}{\alpha \hbar} \right) \times \prod_i \frac{1}{1 + 2\lambda_i} \cdot \exp \left(\frac{2\tilde{V}_i^2}{(1 + 2\lambda_i)} \right),$$

where λ_i are the eigenvalues of the T-matrix and the \tilde{V}_i are the components of the vector V_i in the eigenbasis of the T-matrix. A similar, straightforward calculation also reveals a modification of the average flip probability due to averaging over nuclear spin configurations:

$$\langle P_S \rangle = \frac{\alpha \hbar}{\alpha \hbar + \pi \sum_i B_{i,rms}^2} \exp \left(-\frac{\pi \Omega^2}{2(\alpha \hbar + \pi \sum_i B_{i,rms}^2)} \right). \quad (4)$$

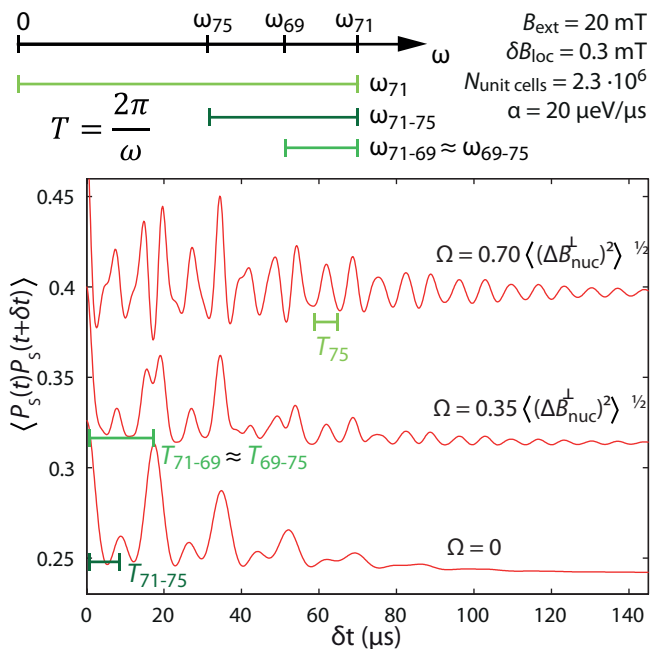


Figure 2. Simulations of correlations for different SO coupling. Above the nuclear spin frequencies are given. For $\Omega = 0$, correlations oscillate with the relative Larmor frequencies. For $\Omega > 0$ additional frequencies appear, and the corresponding oscillations extend to longer times while the original peaks become smaller and some split into two.

For $\Omega = 0$, the behavior changes from exponential to algebraic.

Fig. 2 shows the correlations for typical experimental parameters and different SO coupling constants $\Omega = 0$. As also seen in equation 3, Δ oscillates with the Larmor frequency differences $\omega_i - \omega_j$ for $\Omega = 0$. In GaAs, the three γ_i are approximately equidistant. Therefore, the relative orientations of the three contributions to ΔB_{nuc}^\perp and thus Δ return to nearly the same value after one period $T_{ij} = 2\pi(\omega_i - \omega_j)^{-1}$ of the slower relative precession, $T_{75-69} \approx T_{71-69}$. Hence, large revivals in the correlations occur at this value of δt . The smaller peaks at $\delta t = T_{75-71}$ result from a partial realignment of these two species only. The envelope decay of the correlations on a time scale of approximately $40 \mu s$ arises from nuclear spin dephasing.

As Ω is increased, oscillations at the bare frequencies ω_i extending to larger δt start to appear as well. In addition, the large peak around $\delta t = 17 \mu s$ splits. Observing these features would represent qualitative evidence for SO coupling. At the same time, the magnitude of the variation in the correlations is reduced.

We now turn to proof of principle experimental results, obtained from the same DQD sample as used in [19]. In all measurements, the sweep range was constrained to keep $J(\epsilon) \gg B_{nuc}$ to prevent mixing of S and T_0 . As $B_{ext} \gg \Delta$, the nonlinear sweep and the finite sweep range

do not introduce a large error. A measured background reflecting the direct coupling of the gate pulses to the charge sensor used for single shot readout was subtracted from each dataset.

To verify the expected behavior of flip the probability, we measured its dependence on sweep rate and magnetic field, as shown in Fig. 3(a). The scaling factor used to convert the readout signal to triplet probability was chosen in accordance with the contrast of the (1, 1)-(0, 2) charge transition, taking relaxation during the readout stage into account. The scaling of the x -axis is motivated by the fact that in the experiment the sweeps result in a linear time dependence of ε rather than $J(\varepsilon)$. To compute the sweep rate $\alpha = dJ/dt = dJ/d\varepsilon \cdot d\varepsilon/dt$, we employ the phenomenological relation $J(\varepsilon) = J_0 \exp\left(-\frac{\varepsilon}{\varepsilon_0}\right)$ [21]. At the S-T+ transition, $J(\varepsilon) = B_{\text{ext}}$, so that $\alpha = B_{\text{ext}} \frac{1}{\varepsilon_0} \frac{\Delta\varepsilon}{\Delta t}$, where Δt is time taken to sweep detuning by $\Delta\varepsilon$. Hence, P_S is expected to be a function of $\Delta t/B_{\text{ext}}$, independent of B_{ext} . Indeed, the curves for different B_{ext} in Fig. 3(a) collapse reasonably well onto each other. The deviations for slow sweeps may be a result of relaxation. The solid line was obtained from Eq. 4 using $\Omega = 0$ and a value of Δ^2/α that is a factor 6 smaller than expected based on measurements of T_2^* , from which $N = 2.3 \cdot 10^6$ can be extracted [19]. This adjustment was required to obtain adequate agreement with the model, which contains no further free parameters. As can be seen from the relatively large slope at large Δt , the algebraic dependence obtained from nuclear averaging in equation 4 gives a better overall fit than the exponential LZ formula (dashed line), even if adjusting the scaling factor of the latter.

Guided by these results, we fixed Δt at $0.3 \mu\text{s}$ for the correlation measurements discussed next. Initialization-LZ-sweep-readout cycles as shown in Fig. 1(b) were repeated at a rate of 0.5 MHz. Initialization was carried out via a standard procedure through electron exchange with the leads [2]. Readout was accomplished via RF reflectometry of a quantum point contact [15]. Instead of single shot discrimination, we computed the correlations directly from the readout signal, which was averaged over $1 \mu\text{s}$ in each cycle. Assuming the readout signal is the sum of a contribution from the qubit measurement and noise uncorrelated with the qubit state, this procedure is equivalent to correlating single shot readout values apart from additional noise. Due to the fixed sampling rate, the time resolution was limited to $2 \mu\text{s}$.

The data shown in Fig. 3(b) clearly shows the expected oscillations. For fitting our model to the experiment, only an offset of the QPC signal was adjusted individually for each data set. The y -scale was set analogous to Fig. 3(a). Obtaining good agreement of the magnitude required Δ^2/α to be chosen a factor 18 smaller than expected for $N = 2.3 \cdot 10^6$ unit cells and experimental sweep rates. The δt -dependence is unaffected by this adjustment. Nuclear spin Larmor frequencies were

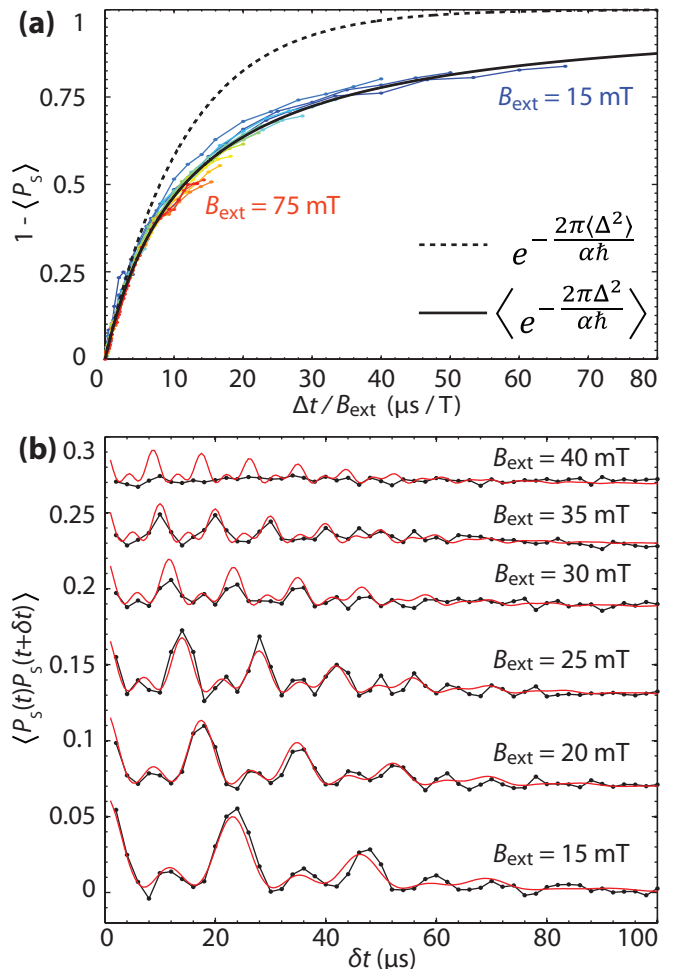


Figure 3. (a) Triplet probabilities as a function of sweep-time Δt from $0 \mu\text{s}$ to $1 \mu\text{s}$ with a constant $\Delta\varepsilon$ for different B_{ext} . The scaling of the time axis with magnetic field leads to a reasonable collapse of the curves. Data in color. The black lines shows the LZ-model (dashed) with a fixed transition matrix element, and the nuclear spin averaged LZ behavior (solid). With $N = 2.3 \cdot 10^6$ fixed, Δ^2/α requires a scaling factor of 6 to match experiment. (b) Correlation of triplet probabilities for different B_{ext} , data in black and model in red. Except for the magnitude, the correlations behave as expected as a function of B_{ext} .

taken from [22]. δB_{loc} determines the time scale of the overall decay and was fixed to 0.33 mT , consistent with earlier measurements [19]. As expected for the low magnetic fields considered here, the effect of SO coupling is negligible. At higher fields, contrast is lost faster than expected from our model, but the time resolution used here also becomes too coarse to resolve the Larmor precession.

The experiments thus confirm the overall picture obtained from our model and the usefulness of single shot correlation measurements. The significant quantitative discrepancy in Δ^2/α is not understood, but may at least partly arise from noise and non-uniformity of the sweep

resulting from the discrete 1 ns sampling interval of the wave form generator. More detailed measurements would be required to explore these effects. By varying the delay between subsequent pulses instead of using a fixed repetition rate, the time resolution could be improved significantly. This would enable an extension to larger magnetic fields where SO coupling might become important.

In conclusion, we have shown that correlation measurements of Landau-Zener sweeps through the S-T+ transition reveal nuclear spin precession and dephasing. These dynamics are seen in an experimental implementation of the scheme. They imply that the perpendicular component of the Overhauser field cannot be controlled as well as the z -component. Our model indicates that the same measurement technique should be able to qualitatively reveal SO coupling at higher magnetic fields.

This work was supported by the Alfried Krupp von Bohlen und Halbach Foundation and DFG under Grant No. BL 1197/2-1. We would like to thank Amir Yacoby, Mark Rudner and Izhar Neder for discussions.

* Present address: QuTech and Kavli Institute of Nanoscience, Delft University of Technology, 2600 GA Delft, The Netherlands

- [1] D. Loss and D. P. DiVincenzo, *Phys. Rev. A* **57**, 120 (1998).
- [2] J. R. Petta, H. Lu, and A. C. Gossard, *Science* **327**, 669 (2010).
- [3] H. Ribeiro, J. R. Petta, and G. Burkard, *Phys. Rev. B* **87**, 235318 (2013).
- [4] H. Ribeiro, G. Burkard, J. R. Petta, H. Lu, and A. C. Gossard, *Phys. Rev. Lett.* **110**, 086804 (2013).
- [5] D. Stepanenko, M. Rudner, B. I. Halperin, and D. Loss, *Phys. Rev. B* **85**, 075416 (2012).
- [6] H. Bluhm, S. Foletti, D. Mahalu, V. Umansky, and A. Yacoby, *Phys. Rev. Lett.* **105**, 216803 (2010).
- [7] S. Foletti, H. Bluhm, D. Mahalu, V. Umansky, and A. Yacoby, *Nature Physics* **5**, 903 (2009).
- [8] C. Kloeffel, P. A. Dalgarno, B. Urbaszek, B. D. Gerardot, D. Brunner, P. M. Petroff, D. Loss, and R. J. Warburton, *Phys. Rev. Lett.* **106**, 046802 (2011).
- [9] C. Latta, A. Hoegele, Y. Zhao, A. N. Vamivakas, P. Maletinsky, M. Kroner, J. Dreiser, I. Carusotto, A. Badolato, D. Schuh, W. Wegscheider, M. Atature, and A. Imamoglu, *Nature Physics* **5**, 758 (2009).
- [10] T. D. Ladd, D. Press, K. De Greve, P. L. McMahon, B. Friess, C. Schneider, M. Kamp, S. Höfling, A. Forchel, and Y. Yamamoto, *Phys. Rev. Lett.* **105**, 107401 (2010).
- [11] M. S. Rudner, I. Neder, L. S. Levitov, and B. I. Halperin, *Phys. Rev. B* **82**, 041311 (2010).
- [12] A. Brataas and E. I. Rashba, *Phys. Rev. B* **84**, 045301 (2011).
- [13] A. Brataas and E. I. Rashba, *Phys. Rev. Lett.* **109**, 236803 (2012).
- [14] I. Neder, M. S. Rudner, and B. I. Halperin, *Phys. Rev. B* **89**, 085403 (2014).
- [15] C. Barthel, D. J. Reilly, C. M. Marcus, M. P. Hanson, and A. C. Gossard, *Phys. Rev. Lett.* **103**, 160503 (2009).
- [16] T. Fink and H. Bluhm, *Phys. Rev. Lett.* **110**, 010403 (2013).
- [17] L. Landau, *Physics of the Soviet Union 2*, 46 (1932).
- [18] C. Zener, *Proc. Roy. Soc. London, Ser. A* **137**, 696 (1932).
- [19] H. Bluhm, S. Foletti, I. Neder, M. Rudner, D. Mahalu, V. Umansky, and A. Yacoby, *Nature Physics* **7**, 109 (2011).
- [20] I. Neder, M. S. Rudner, H. Bluhm, S. Foletti, B. I. Halperin, and A. Yacoby, *Phys. Rev. B* **84**, 035441 (2011).
- [21] O. E. Dial, M. D. Shulman, S. P. Harvey, H. Bluhm, V. Umansky, and A. Yacoby, *Phys. Rev. Lett.* **110**, 146804 (2013).
- [22] D. Paget, G. Lampel, B. Sapoval, and V. I. Safarov, *Phys. Rev. B* **15**, 5780 (1977).